

Supplementary Information

***In-situ* observation of carrier transfer in Mn-oxide/Nb:SrTiO₃ photoelectrode by X-ray absorption spectroscopy**

Masaaki Yoshida,^{*,a} Takumi Yomogida,^a Takehiro Mineo,^a Kiyohumi Nitta,^b Kazuo Kato,^b Takuya Masuda,^c Hiroaki Nitani,^d Hitoshi Abe,^d Satoru Takakusagi,^e Tomoya Uruga,^b Kiyotaka Asakura,^e Kohei Uosaki,^{c,f,g} and Hiroshi Kondoh,^{*,a}

^a Department of Chemistry, Keio University, Yokohama, Japan

^b Japan Synchrotron Radiation Research Institute, Hyogo, Japan

^c Global Research Center for Environment and Energy based on Nanomaterials Science, National Institute for Materials Science (NIMS), Ibaraki, Japan

^d Institute of Materials Structure Science, KEK, Ibaraki, Japan

^e Catalysis Research Center, Hokkaido University, Sapporo, Japan,

^f International Center for Materials Nanoarchitectonics (WPI-MANA), NIMS, Ibaraki, Japan

^g Graduate School of Chemical Sciences and Engineering, Hokkaido University, Sapporo, Japan

*E-mail: yoshida@chem.keio.ac.jp; kondoh@chem.keio.ac.jp

Index	Page
Experimental procedures	S2
Schematic illustration of optical geometry for <i>in situ</i> XAFS measurements	S5
Evolution of gases	S6
<i>In situ</i> XAFS spectra at various potentials	S7
Relation between Mn valence and absorption edge energy	S9
Photocurrent monitored during <i>in situ</i> XAFS measurement	S10
Time course of <i>in situ</i> XAFS spectra after changing potential	S11
Difference between the thin film and particle samples	S12
Reference	S13

Experimental procedures

Preparation of samples. Nb:SrTiO₃ substrates (10×10 mm²) with polished surfaces were purchased from Furuuchi Chemical Co.. The Nb:SrTiO₃ substrates were suspended in an aqueous solution of Mn(NO₃)₂·6H₂O (98%, Kanto Chemicals) (2.2×10⁻² mol/L) and irradiated with a Xe lamp (300 W, Cermax) for photodeposition of the Mn oxide cocatalysts. The amounts of photodeposited Mn oxide were controlled by changing the photon intensity of UV irradiation as ca. 10¹⁶ photons·s⁻¹·cm⁻² for particulate sample and ca. 10¹⁸ photons·s⁻¹·cm⁻² for thin film sample. The surface morphology of Nb:SrTiO₃ substrates was observed by atomic force microscopy (AFM; SPM-9500J3, Shimadzu), which indicated that the Mn oxide cocatalysts were photodeposited as particles or thin film on the Nb:SrTiO₃ substrates. A Cu wire was connected to the prepared samples with Ag paste and placed in a Teflon electrochemical cell sealed with epoxy resin, as working electrodes.

Photoelectrochemical reaction. The Teflon electrochemical cell was equipped with a Pt wire counter electrode, an Ag/AgCl (saturated KCl) reference electrode, and the prepared sample as the working electrode. The photoelectrochemical reaction of the samples for O₂ evolution from an aqueous solution of 0.1 M Na₂SO₄ (99.99%, Merck) bubbled with Ar was performed using a potentiostat (HA-151B, Hokuto Denko Co.) to control the electrode potential. A 300 W Xe lamp with an IR-cut filter was used for UV irradiation through the polypropylene window (12.0 μm, Chemplex Industries Inc.). Milli-Q water (total organic carbon < 5 ppb, resistivity > 18 MΩ cm) was used in all the experiments. The time sequences of the potential or current were obtained with an AD converter (USB-6211, National Instruments) and recorded in a personal computer after averaging 100 values collected at a sampling rate of 100 kHz using the LabVIEW program (National Instruments).

Detection of evolved gases. The prepared samples were set in an aqueous solution of 0.1 M Na₂SO₄ using a Pyrex reaction vessel covered with a Teflon plate connected to a stainless closed-gas system, a Pt wire counter electrode, an Ag/AgCl (saturated KCl) reference electrode, and the prepared sample as

the working electrode. After the reactant solution was evacuated several times to completely remove air, Ar gas was supplied into the reaction system. A potentiostat was used to control the electrode potential. Irradiation was conducted using a 300 W Xe lamp with an IR-cut filter. The gases evolved during the reaction were analyzed using a quadrupole mass spectrometer (M-070QA-TDF, Canon Anelva Co.).

***In situ* XAFS.** XAFS spectra were obtained at BL-12C of the Photon Factory (PF) using an electron energy of 2.5 GeV with an average current of 450 mA, and at BL01B1 of SPring-8 using an electron energy of 8.0 GeV with an average current of 100 mA. The radiation was monochromatized with a Si(111) double-crystal monochromator. The intensities of the incident X-rays were monitored using ion chambers filled with a gas mixture of N₂ (30%) and He (70%) in front of the sample for I₀ (17cm long), and with a gas mixture of N₂ (85%) and Ar (15%) after the sample for I₁ (31 cm long). The MnO (99%, Strem Chemicals), Mn₃O₄ (99.9%, Soekawa Chemicals), Mn₂O₃ (99%, Strem Chemicals), MnO₂ (>85%, Wako), and KMnO₄ (99.3%, Wako) reference samples were diluted in boron nitride (1% w/w) and placed in a paper holder sealed with scotch tape. Data for the prepared samples were collected as fluorescence excitation spectra with 19 element Ge detectors (PF:Ortec, SPring-8:Canberra) equipped with a 3- μ m Cr filter and solar slits to eliminate scatter. Analysis of the raw XAFS spectra was conducted using the Athena and Artemis programs¹. The photon energies were calibrated according to the X-ray absorption edge of Mn foil (6537.0 eV). The Teflon electrochemical cell was equipped with a Pt wire counter electrode, an Ag/AgCl (saturated KCl) reference electrode, and the sample connected to a Cu wire with Ag paste as the working electrode. The X-ray beam was irradiated at an incident angle of 4° through the polypropylene window (12.0 μ m thick). A potentiostat was used to control the electrode potential in an Ar-saturated aqueous solution of 0.1 M Na₂SO₄. Milli-Q water (total organic carbon < 5 ppb, resistivity > 18 M Ω cm) was used in all the experiments. The time sequences of the potential or current values were obtained using an AD converter and recorded in a personal computer after averaging 100 values collected at a sampling rate of 100 kHz. XAFS spectra of the prepared samples were measured at various potentials under dark conditions and under UV irradiation with a Xe lamp

equipped with a cold mirror, an IR-cut filter, or a neutral density filter. The aqueous solutions in the measurement cell kept almost the same temperature between before and after photoirradiations. The intensities of the incident X-rays to samples (ca. 10^9 photons·s⁻¹) were much less than these of the UV irradiation (ca. 10^{16} photons·s⁻¹) by the rough estimation, resulting in that the radiation damage by the incident X ray was not observed in our experiment.

Schematic illustration of optical geometry for in situ XAFS measurements

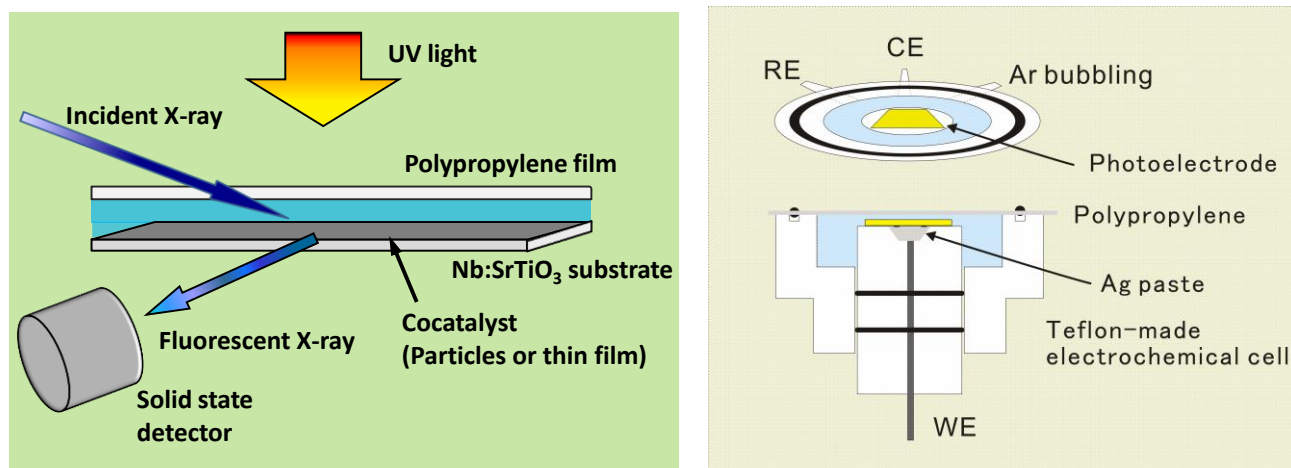


Figure S1. Schematic illustration of the optical geometry and electrochemical cell for *in situ* XAFS measurements. A Teflon electrochemical cell was used with a Pt wire counter electrode, an Ag/AgCl (saturated KCl) reference electrode, and a prepared sample connected to a Cu wire with Ag paste as the working electrode, in an Ar-saturated aqueous solution of 0.1 M Na₂SO₄. A Xe lamp was used for UV irradiation.

Evolution of gases

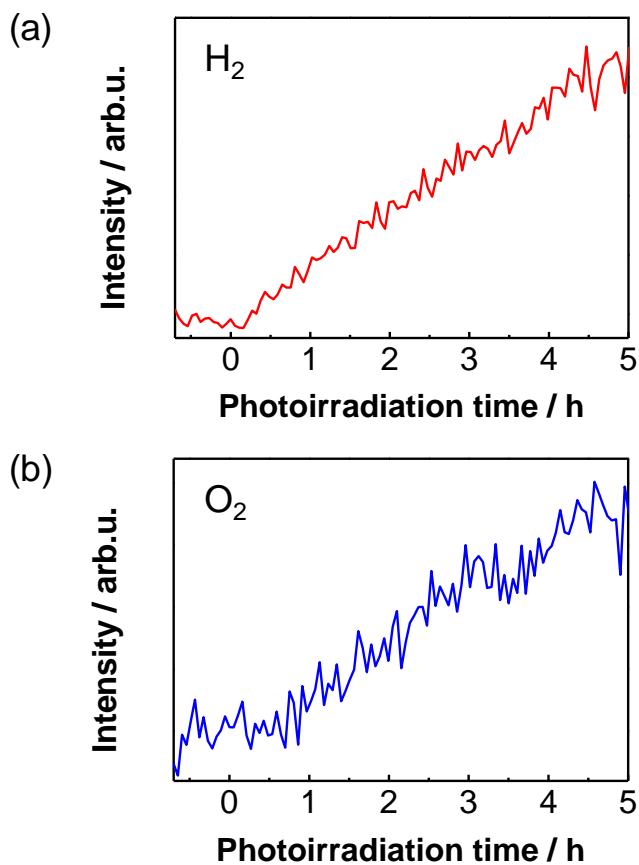


Figure S2. Change in mass peak intensities of hydrogen (a) and oxygen (b) gases. The gases evolved via photoelectrochemical reaction with the Mn-oxide-particle/Nb:SrTiO₃ photoelectrode for the water splitting reaction from an Ar-saturated aqueous solution of 0.1 M Na₂SO₄ at 1.0 V vs. Ag/AgCl under UV irradiation.

In situ XAFS spectra at various potentials

First, we checked potential dependence of the Mn oxide deposited on the photoelectrode without UV irradiation. Figure S3a shows Mn K-edge XAFS spectra for the thin film Mn oxide on the Nb:SrTiO₃ photoelectrode measured under various controlled potentials between -1.5 and 1.5 V vs. Ag/AgCl, together with those for the MnO, Mn₃O₄, Mn₂O₃, MnO₂, and KMnO₄ model compounds. The edge position of each model compound is shifted to higher energy with increase in the formal oxidation state. At a potential of -1.5 V, the peak position for Mn-oxide/Nb:SrTiO₃ (6556.9 eV) is similar to that for the Mn₃O₄ and Mn₂O₃ reference samples (6557.0 and 6556.9 eV), which indicates that the electronic structure of the Mn oxide species is most likely the same as that of Mn³⁺. As the potential was changed from -1.5 to 1.5 V, the peak position was gradually shifted to higher energy until -0.5 V and then remained constant at 6558.2 eV until 1.5 V, which shows the Mn oxide species was oxidized to some extent by positive electrode potential. Therefore, the result implies that the electronic structure of the Mn oxide species can change by electron migration between Nb:SrTiO₃ substrate and Mn oxide cocatalyst. It should be noted that the electron migration can be restricted due to upward band bending derived from the n-type semiconductor characteristics.²

To further examine the effect of the surface morphology of the Mn oxide, XAFS spectra of the Mn oxide particle sample were measured under potential control between -1.0 and 1.0 V (Figure S3b). At -1.0 V, the peak for the Mn species was observed at 6550.9 eV, which corresponds with that for the MnO reference sample (6552.7 eV) and indicates that the valence state of Mn in the Mn oxide particles is most likely Mn²⁺. As the potential was changed from -1.0 to 1.0 V, the peak shifted to higher energy at 6557.8 eV. This peak position is coincident with that for the Mn₃O₄ and Mn₂O₃ reference samples (6557.0 eV or 6556.9 eV, respectively), which implies that the valence state of Mn in the Mn oxide particles can change between Mn²⁺ and Mn³⁺. The Mn²⁺ species has been reported to dissolve in electrolyte solutions.³ In the present measurements, the whole spectrum intensity decreased by half for 3 hours when the Mn²⁺ species was formed. However, Mn³⁺ species is considerably stable in water and

does not decrease before photoirradiation. Thus, in Figure 2, the decrease of Mn^{3+} species under photoirradiation is due to the formation of Mn^{2+} species by reduction of Mn^{3+} species using photogenerated electron, because the valence state of Mn in the Mn oxide particles can be changed between Mn^{2+} and Mn^{3+} by the applied electrode potential, as shown in Figure S3b.

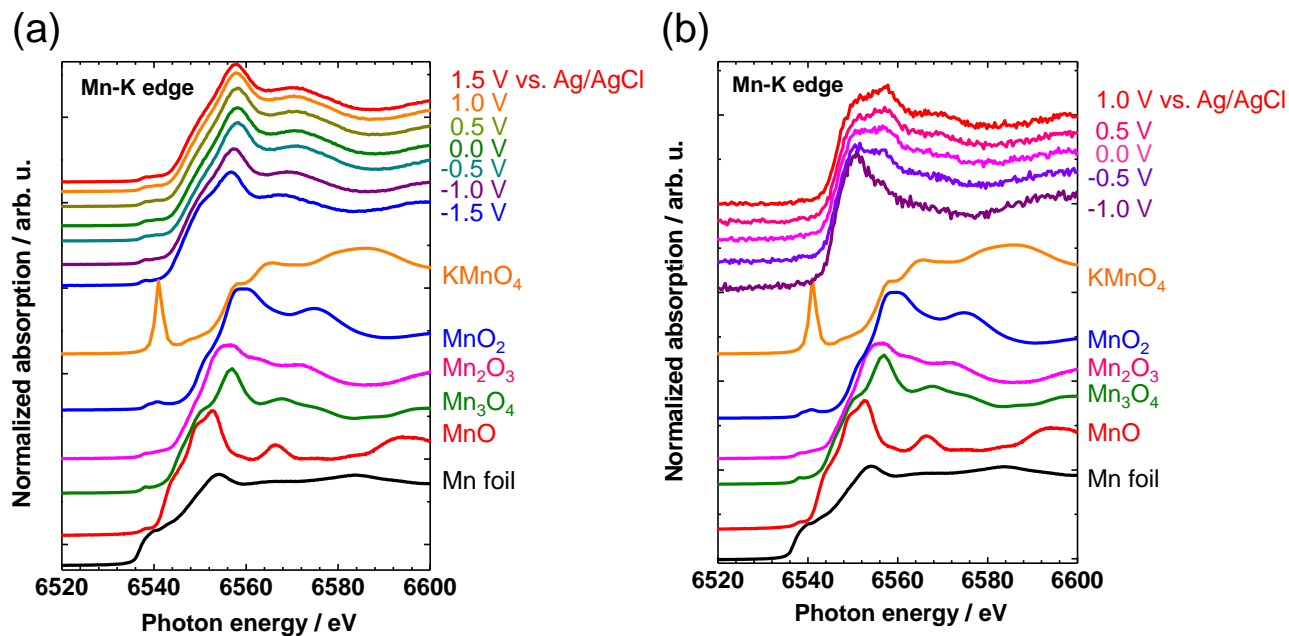


Figure S3. Mn K-edge XAFS spectra for the Mn oxide (a) thin film and (b) particles on the Nb:SrTiO_3 photoelectrodes at various applied potentials in an Ar-saturated aqueous solution of 0.1 M Na_2SO_4 without UV irradiation. XAFS spectra for Mn foil, MnO, Mn_3O_4 , Mn_2O_3 , MnO_2 , and KMnO_4 are shown for reference.

Relation between Mn valence and absorption edge energy

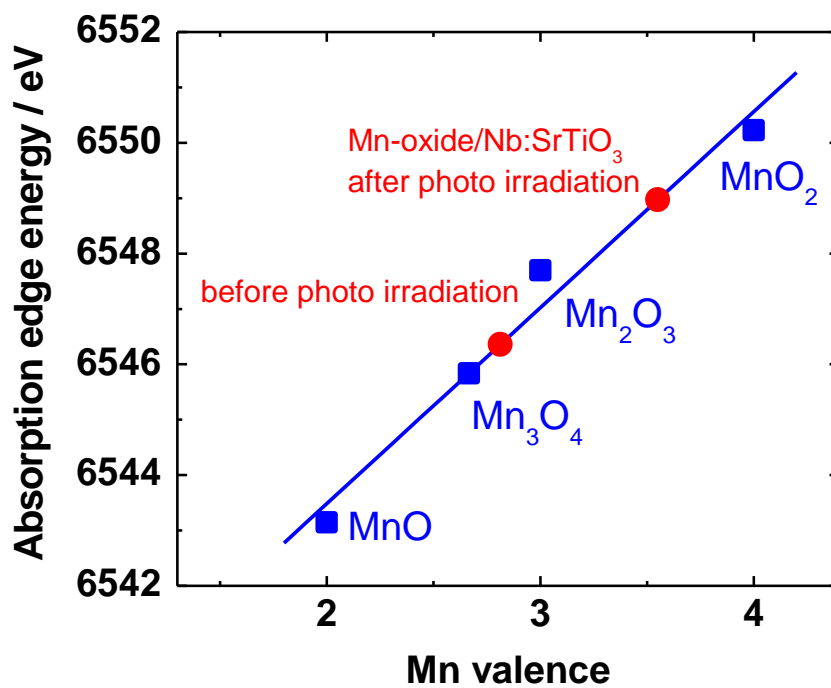


Figure S4. Relation between Mn valence and absorption edge energy estimated as the half-way point of the absorption of the references and the Mn oxide thin film on the Nb:SrTiO₃ photoelectrode. The oxidation states of samples were determined using the Mn K-edge energy shift of the reference Mn compounds.

Photocurrent monitored during in situ XAFS measurement

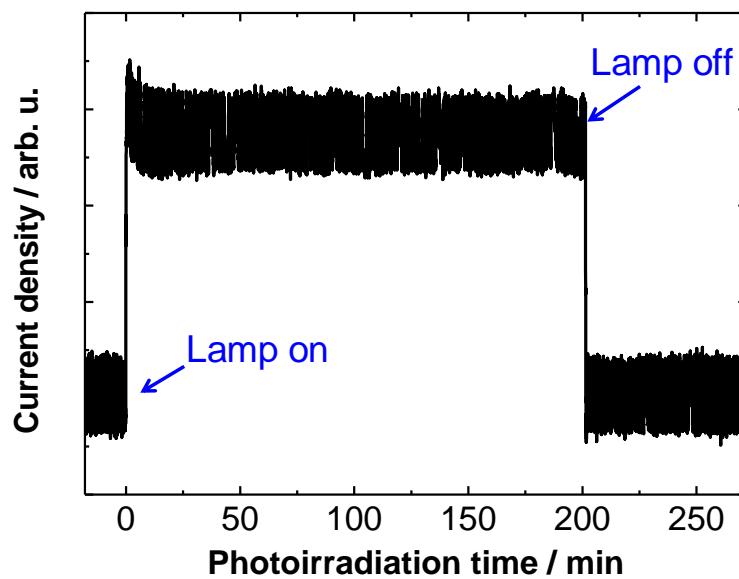


Figure S5. Change in oxygen evolution current density for the Mn-oxide-deposited Nb:SrTiO₃ photoelectrode in Ar-saturated aqueous solution of 0.1 M Na₂SO₄.

Time course of in situ XAFS spectra after changing potential

It is reported that carrier injection at the cobalt-phosphate/ Fe_2O_3 interface is fast, in a range from microseconds to seconds, by probing the photogenerated carrier behavior in the semiconductor photoelectrode.³ In contrast, the electronic state change of Mn oxide cocatalysts on the photoelectrode in this work was much slower with a time scale of ca. 2 h, meaning that the amount of hole transfer is over 100 times more than that of Mn atoms on the Nb:SrTiO₃ substrate by a rough estimation, as shown in Figure 2. On the other hand, the change of XAFS spectra by photoirradiation is similar with that by drastic potential change from 0.0 V to 1.0 V, as shown in Figure S6. Therefore, we suggest that the XAFS spectrum does not directly trace the decay of the photogenerated carrier, but indicates the relaxation behavior toward an electrochemical quasi-equilibrium induced by the potential change from the accumulation of competitive electron or hole migrations from the Nb:SrTiO₃ photoelectrode to the Mn oxide cocatalyst.

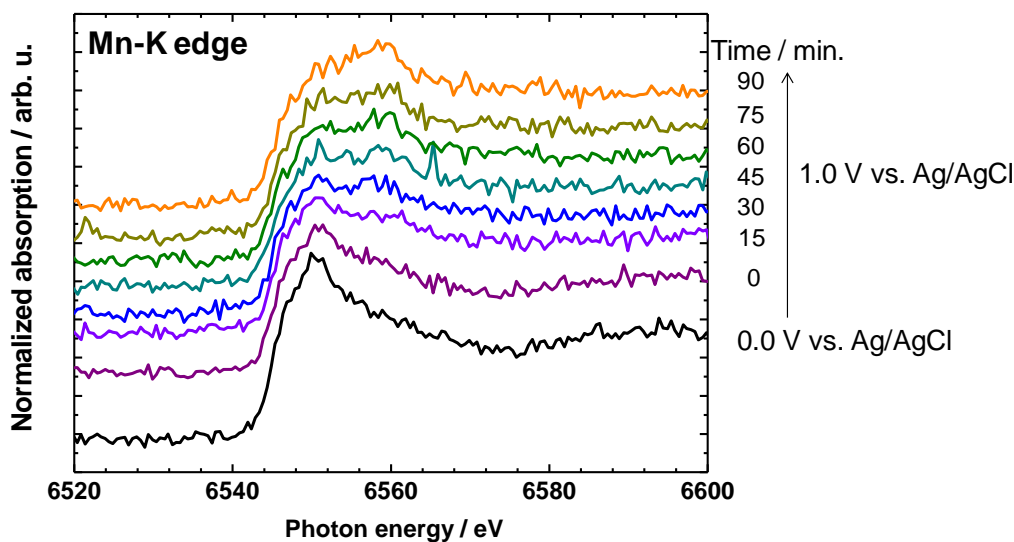


Figure S6. Time course of *in situ* Mn K-edge XAFS spectra for the Mn-oxide-particle/Nb:SrTiO₃ electrode in an Ar-saturated aqueous solution of 0.1 M Na₂SO₄ with change in the potential from 0.0 to 1.0 V.

Difference between the thin film and particle samples

The existence of reduced and oxidized Mn oxide in the particulate sample means that the potential of each Mn oxide particle is not homogeneous. We guess that the irregularity is owing to the electron migration can be restricted due to upward band bending derived from the n-type semiconductor characteristics of Nb:SrTiO₃ single crystal substrate. The individual Mn oxide particles do not have electrical conductivity with each other. Thus, even if some Mn oxide particles were reduced, the other particles are likely to keep the different potential. On the contrary, the thin film sample is homogeneous in view of the electrical conductivity, which results in that the whole Mn oxide species was oxidized.

References

- 1 (a) M. Newville *Journal of synchrotron radiation*, 2001, **8**, 322. (b) B. Ravel and M. Newville *Journal of synchrotron radiation*, 2005, **12**, 537.
- 2 M. Yoshida, A. Yamakata, K. Takanabe, J. Kubota, M. Osawa and K. Domen *J. Am. Chem. Soc.*, 2009, **131**, 13218.
- 3 M. Barroso, A. J. Cowan, S. R. Pendlebury, M. Gratzel, D. R. Klug and J. R. Durrant *J. Am. Chem. Soc.*, 2011, **133**, 14868.